

# Peak and history effects in two-dimensional collective flux pinning

R. Wördenweber and P. H. Kes

*Kamerlingh Onnes Laboratory, University of Leiden, P.O. Box 9506, 2300 RA Leiden, The Netherlands*

C. C. Tsuei

*IBM Thomas J. Watson Research Center, P.O. Box 218, Yorktown Heights, New York 10598*

(Received 16 July 1985)

Flux pinning in amorphous  $\text{Nb}_3\text{Ge}$  and  $\text{Mo}_3\text{Si}$  films with thicknesses ranging from 60 nm to 3  $\mu\text{m}$  has been studied as a function of perpendicular field, temperature, and history of the flux-line lattice (FLL). The theory of two-dimensional collective pinning agrees well with the critical-current data up to the field  $B_{ST}$ . Between  $B_{ST}$  and  $B_{c2}$  a peak effect is observed for which possible origins are discussed in detail. It is concluded that elastic instabilities generated by local fluctuations of the pinning force on individual vortices induce a structural transition (ST) of the FLL at  $B_{ST}$ . A theoretical criterion derived for  $B_{ST}$  is in good agreement with the data. Isofield experiments clearly show for the first time the presence of flux-line dislocations in the peak regime. They cause an enhancement of the pinning force by the local reduction of the shear modulus. In the field region around  $B_{ST}$  distinct effects of the formation history of the FLL are observed. It is shown that the FLL can exist in metastable states which structurally relax upon a sufficiently fast movement of the lattice past the pinning centers.

## I. INTRODUCTION

Considerable progress has recently been made concerning the long-standing problem of the summation of forces exerted by individual pinning centers (pins) on the flux-line lattice (FLL) of a type-II superconductor in the mixed state.<sup>1,2</sup> It has also been recognized that the approach<sup>3-5</sup> in which the individual pins contribute independently to the volume pinning force  $F_p = BJ_c$ , where  $J_c$  is the critical-current density, is not representative for most real pinning systems.<sup>6</sup> Because of the large densities of pins,  $n_v$ , and the small elementary interaction forces  $f$ , only the collective action of the pins is significant. Larkin and Ovchinnikov<sup>1</sup> (LO) showed that the long-range positional order is destroyed and for the case of elastic deformation they derived expressions for the transverse and longitudinal correlation lengths,  $R_c$  and  $L_c$ , that determine the length scales over which the FLL is still correlated. In addition, they modelled the FLL as being divided into elastically independent domains, the correlated regions, with a volume  $V_c \approx R_c^2 L_c$ . The net pinning force on a correlated region depends on the statistical fluctuations expressed by  $(n_v V_c \langle f^2 \rangle)^{1/2}$ . The volume pinning force is therefore

$$J_c B = [W(0)/V_c]^{1/2} \quad (1)$$

with

$$W(0) = n_v \langle f^2 \rangle. \quad (2)$$

The case of two-dimensional collective pinning (2D CP) occurs when  $L_c$  is much larger than the sample thickness  $d$ , so that  $V_c \approx R_c^2 d$ . 2D CP has been experimentally verified by Kes and Tsuei<sup>7</sup> on thin amorphous films of  $\text{Nb}_3\text{Ge}$ ,  $\text{Nb}_3\text{Si}$ , and  $\text{Mo}_3\text{Si}$  up to a certain reduced magnetic field  $b_{ST}$  (Ref. 8) (see also Fig. 1 of this paper), which

marks a structural transition (ST). Below  $b_{ST}$  a scaling law is found for all temperatures and all samples, which is in excellent agreement with the theory. However, above  $b_{ST}$  the pinning force exhibits a deviating peak which is accompanied by history effects in the field region around  $b_{ST}$ . Typical 2D CP behavior has now been observed in films of amorphous Zr-Si alloys,<sup>9</sup>  $\alpha\text{-Mo}_5\text{Ge}$ ,<sup>10</sup> and melt-spun  $\alpha\text{-Zr}_{70}\text{Cu}_{30}$ .<sup>11</sup> In the latter case a large peak is also found at low fields. It decreases after annealing.<sup>11</sup> An extensive comparison of the 3D CP theory with experiments by Kerchner<sup>2</sup> shows qualitative agreement, especially regarding the quadratic dependence of  $F_p$  on  $W(0)$ . Recent experimental work on irradiated Nb and  $\text{Nb}_{80}\text{Ta}_{20}$  (Ref. 12) and on  $\text{V}_3\text{Si}$  crystals (Ref. 13) further confirms this feature of the 3D CP theory. The 3D CP theory for an amorphous FLL near  $B_{c2}$  has been applied to study the elementary pinning interaction of voids in Nb and V.<sup>14</sup>

The purpose of the present work is to explore the physics behind the peak effect and related history effects for the case of 2D CP in particular. In the past, these subjects have been studied by many authors,<sup>15,16</sup> and several models have been suggested for the peak effect. The common property of these models is the softening of the FLL either because near  $B_{c2}$  the shear modulus  $c_{66}$  decreases faster than  $f_p$ ,<sup>17</sup> or because of the dispersive behavior of the tilt modulus  $c_{44}$ .<sup>1,5</sup> In two-dimensional systems only the first mechanism can be responsible. The following question therefore remains: Which mechanism causes the softening of the FLL? In a detailed analysis given in Sec. III we consider four possibilities.<sup>18</sup>

- (1) A dimensional crossover from 2D to 3D CP when  $L_c$  becomes smaller than  $d$ .
- (2) A sudden increase of  $W(0)$ .
- (3) Local elastic instabilities cause a *structural transition*

of the FLL from an elastically distorted lattice below  $b_{ST}$  to a plastically distorted lattice above  $b_{ST}$ . This decreases the volume of the correlated regions and enhances the pinning.<sup>19</sup>

(4) The shear strength of the FLL is exceeded at  $b_{ST}$ , which also initiates a transition from elastic to plastic behavior.

In Sec. IV we describe new experiments that provide definite evidence for a structural transition. They show that an amorphous FLL very close to  $B_{c2}$  is attained via a vortex structure in which the pinning is determined by flux-line defects,<sup>20</sup> e.g., flux-line dislocations (FLD's), stacking faults, etc.<sup>21</sup> When the magnetic field approaches  $B_{c2}$ , Mullock and Evetts demonstrated very recently<sup>22</sup> that a defective vortex lattice modelled by a square array of dislocations can indeed represent an equilibrium state of lower energy than the elastic solution derived by LO. History effects as well as transient flux-flow phenomena<sup>23</sup> are generally supposed to be related to the plasticity of the FLL.<sup>16</sup> In Sec. IV B it is discussed that the history and relaxation effects we observe can be well explained in terms of FLD's.

## II. SAMPLE PREPARATION AND EXPERIMENTAL PROCEDURES

The amorphous Nb<sub>3</sub>Ge films are deposited on sapphire substrates by rf sputtering. Variations in most of the sputter parameters such as sputter rate (0.2–0.5 nm/s), substrate temperature during sputtering (LN<sub>2</sub> or water cooled), or the sputter gas (Kr or Ar) do not influence the main features of the samples. Only the purity of the sputter atmosphere and of the target material is essential for the quality of the film. The composition of some of the samples was measured by electron microprobe analysis. No detectable amounts of materials other than Nb and Ge could be traced. The amorphous nature of the sample was checked by x-ray diffraction experiments. A special treatment was given to sample No. 2. It was annealed for 48 hours at 580°C ( $T_{\text{glass}} \approx 750^\circ\text{C}$ ) and subsequently bombarded with Ar ions. Since amorphous Nb<sub>3</sub>Ge is a weak-coupling type-II superconductor in the extreme dirty limit,<sup>24</sup> we can calculate the important superconducting parameters from well-known theoretical expressions<sup>7</sup> (see Table I).

For the pinning-force measurements a standard four-probe technique was used. The critical current  $I_c$  was defined by a voltage drop of 1  $\mu\text{V}$  over a sample length of 6

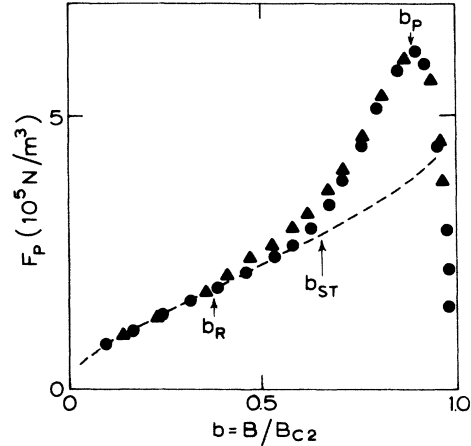


FIG. 1. Volume pinning force of Nb<sub>3</sub>Ge, sample No. 6 at  $t = 0.7T_c$  vs  $b$  for increasing (circles) and decreasing (triangles) field. The dashed line represents the 2D LO theory. Below  $b_R$  history effects are absent. Above  $b_{ST}$  the data deviate from theory (peak effect), at  $b_p$   $F_p$  is maximum.

mm. We used two different methods to measure  $I_c$ . In the *current-sweep* (CS) method we kept the temperature and magnetic field at a constant value and measured the  $I$ - $V$  curve. From this curve not only could the values for  $I_c$  and the flow resistance be obtained, but it also gave insight into structural relaxation processes of the FLL. In the *constant-voltage* (CV) method we kept the voltage at a constant value of 1  $\mu\text{V}$  and varied the temperature or field while recording  $I_c$ . Path dependences of the pinning force, which have their origin in the structure of the unrelaxed FLL, could be immediately depicted in this way.

## III. ORIGIN OF THE PEAK EFFECT

A typical result of an isothermal, static measurement is given in Fig. 1. The volume pinning force  $F_p$  is plotted versus the reduced field  $b = B/B_{c2}$ . For comparison we have added the curve determined with the 2D CP theory. In increasing field up to a value  $b_{ST}$  the pinning force coincides with the prediction of the LO theory.<sup>7</sup> A distinct field-history dependence is observed in decreasing the magnetic field between  $b_{ST}$  and  $b_R$ . Reversible behavior is found below  $b_R$ . History effects will be thoroughly described in Sec. IV. Above  $b_{ST}$  the values found for  $F_p$  are essentially higher than those predicted by LO. The smoothness of the transition at  $b_{ST}$  depends

TABLE I. Properties of the amorphous samples.

Material	Sample No.	$d$ ( $\mu\text{m}$ )	$T_c$ (K)	$\Delta T_c$ (mK)	$\rho_0$ ( $\mu\Omega\text{m}$ )	$-\mu_0 dH_{c2}/dT _{T_c}$ (T/K)	$\kappa$	$\xi(0)$ (nm)	$\lambda(0)$ ( $\mu\text{m}$ )	$B_{c2}(0)$ (mT)
Nb <sub>3</sub> Ge	1	2.92	4.25	170	1.65	1.83	61	6.5	0.65	52
Nb <sub>3</sub> Ge	2	1.24	3.81	71	1.65	1.67	57	7.3	0.68	44
Nb <sub>3</sub> Ge	3	0.62	3.86	10	1.64	2.04	65	6.5	0.68	50
Nb <sub>3</sub> Ge	4	0.46	4.00	12	1.66	1.97	64	6.4	0.68	50
Nb <sub>3</sub> Ge	5	0.06	3.32	40	1.59	1.33	52	8.6	0.73	35
Nb <sub>3</sub> Ge	6	0.17	3.49	12	1.63	1.39	53	8.2	0.72	37
Nb <sub>3</sub> Ge	7	0.093	3.00	17	1.79	1.61	58	8.6	0.82	32
Mo <sub>3</sub> Si	8	0.34	7.06	98	1.7	2.04	65	4.8	0.51	89

on the homogeneity and the thickness of the sample. At the peak ( $b = b_p$ )  $R_c$  approaches the lattice parameter  $a_0$ ,<sup>7</sup> so that the FLL structure becomes amorphous. For  $b > b_p$  the pinning force is then given by

$$F_p = [W(0)/dR_c^2(b_p)]^{1/2},$$

which agrees with the linear decrease  $\propto 1 - b$  between  $B_p$  and  $B_{c2}$ .

In the following we discuss the possible explanations of the peak effect as mentioned in Sec. I. A criterion for the onset of the peak is derived and compared with our experimental results.

#### A. Dimensional crossover

The action of many randomly distributed point pins generally causes shear, tilt, and compressional distortions of the FLL. This also holds for thin-film superconductors in a perpendicular field, in which case, however, due to the incompressibility,<sup>25</sup> the compressional or tensile deformations play no role. There still remain shear and tilt deformations, but if both the pinning is weak and the thickness small, no sufficient disorder develops to disturb the long-range order of the FLL along the field direction, and one may consider the flux lines to be straight and parallel, ignoring the small-scale tilt distortions. This is the case for two-dimensional pinning, theoretically denoted by the condition  $L_c > d/2$ ,<sup>26</sup> where  $L_c$  is related to  $R_c$  by the ratio  $(c_{44}/c_{66})^{1/2}$ . Since Brandt's work,<sup>25</sup> it is known that the tilt modulus is dispersive, leading to a notable reduction of  $c_{44}$  when  $B_{c2}$  is approached. It has been suggested that this effect is responsible for the peak effect in three-dimensional pinning.<sup>1,5</sup> It might as well be the reason for the peak we observed.<sup>7,27</sup>

To establish that we have true two-dimensional pinning for  $b < b_{ST}$  we plotted  $F_p(t=0.7, b=0.4)/B_c^2(t=0.7)$  versus  $1/d$ . As discussed in Ref. 7, the product of  $F_p$  and  $d$  at constant  $t$  and  $b$  only depends on the superconducting bulk properties and the pinning mechanism of the samples. As to the first, variations are mainly accounted for by the factor  $B_c^{-2}(t)$ . Therefore, films with the same alloy composition and the same preparation method should show a linear relationship between  $F_p$  and  $d$ . This

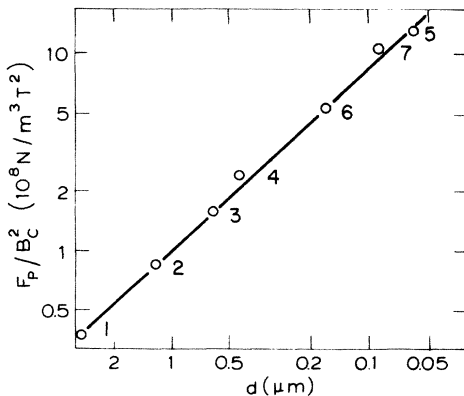


FIG. 2. Double logarithmic plot of  $F_p/B_c^2$  vs  $d$  at  $b=0.4$  and  $t=0.7$  for  $\text{Nb}_3\text{Ge}$  films. The factor  $B_c^{-2}$  accounts for small variation in the superconducting parameters of our samples such as  $T_c$  or  $B_{c2}$ .

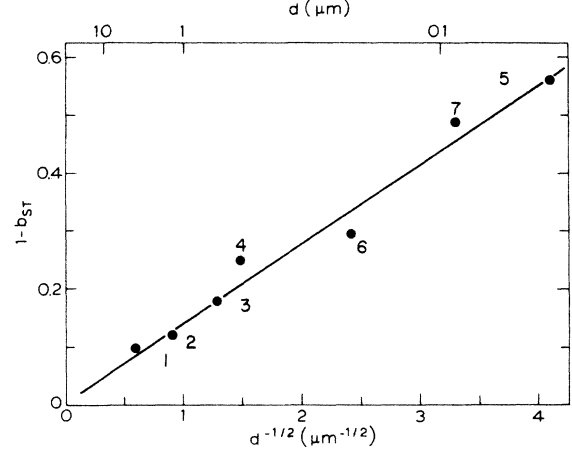


FIG. 3. Plot of  $1 - b_{ST}$  vs  $d^{-1/2}$  for  $\text{Nb}_3\text{Ge}$  films at  $t=0.7$ . The  $d^{-1/2}$  dependence of  $1 - b_{ST}$  at a given temperature directly follows from Eqs. (5), (6), and (10). The slope of this plot yields a value of about 17 for  $R_c/a_0$  at  $b_{ST}$ .

was found for our samples (Fig. 2), proving the two-dimensional nature of the flux pinning below  $b_{ST}$ . In addition, it reveals the uniformity of our samples.

From Eq. (50) of Ref. 1 it is anticipated that the appropriate expression for  $L_c$  is

$$L_c = (c_{44}/c_{66})^{1/2} R_c \quad (3)$$

with (for large  $\kappa$ , without dispersion, at small  $b$ )<sup>28</sup>

$$c_{44} \approx B^2/\mu_0 \quad (4a)$$

and<sup>28</sup> (with dispersion,  $b > 0.5$ )

$$c_{44} \approx B^2(1-b)/\mu_0 \kappa^2. \quad (4b)$$

The 2D CP expression for  $R_c$  is<sup>7</sup>

$$R_c = \left[ \frac{2\pi}{\ln(w/R_c)} \frac{a_0^2 c_{66}^2 d}{W(0)} \right]^{1/2} \quad (5)$$

with  $w$  the width of the sample (4 mm).

The field dependence of  $c_{66}$  and  $W(0)$  is  $\propto b(1-b)^2$ , which leads to  $L_c \propto b^{1/2}$  (no dispersion) and  $L_c \propto b^{1/2}(1-b)^{1/2}$  (with dispersion). Due to the softening of  $c_{44}$ ,  $L_c$  shrinks when  $B_{c2}$  is approached. At  $L_c \approx d/2$  a transition to 3D CP occurs. Evidently, the dimensional crossover is expected closer to  $B_{c2}$  for the thinner samples. Our experiments just show the opposite behavior,  $b_{ST}$  decreases with decreasing thickness  $d$  (Fig. 3). A dimensional crossover is therefore ruled out as a mechanism for the peak effect.

Additionally,  $L_c$  can be determined from Eqs. (3) and (4) for the 2D case both with dispersion ( $\tilde{L}_c^{2D}$ ) and without dispersion ( $L_c^{2D}$ ) and in the case of 3D CP from Eq. (50) of Ref. 1 ( $\tilde{L}_c^{3D}$ ). Using the value

$$W(0) = (4.3 \times 10^{-7}) b(1-b)^2 N^2/m^3,$$

experimentally obtained for sample No. 2 at  $0.7T_c$ , we find  $\tilde{L}_c^{3D}/d \sim 10^6$ ,  $L_c^{2D}/d \sim 10^3$ , and  $\tilde{L}_c^{2D}/d \sim 10$  for  $b$  between 0.1 and 0.95. Mathematically,  $\tilde{L}_c^{3D}$  should decrease for  $b \rightarrow 1$ , but this happens so close to  $B_{c2}$  that the dispersion does not contribute in practice. Because  $\tilde{L}_c^{2D}$

is of the order of 10  $\mu\text{m}$ , crossover effects may be observed for very thick sputtered films. Work on the dimensional crossover is in progress both experimentally and theoretically.<sup>26</sup> It is clear, however, that for  $d < 3 \mu\text{m}$ , it cannot be the reason for the peak effect.

### B. Enhancement of $W(0)$

$W(0)$  is determined by  $n_v$  and the squared actual elementary interaction averaged over a lattice cell. In our amorphous samples the pinning is caused by stress and density fluctuations on a length scale of the order of  $\xi$ . This leads to<sup>7,29,30</sup>

$$W(0) = C_{dl}(T)b(1-b)^2, \quad (6)$$

giving good agreement between experiment and theory up to  $b_{ST}$ .

A sudden enhancement of the elementary interaction itself can be ruled out. Therefore, it might be the violation of the concepts under which  $W(0)$  appears in the theory. As was first pointed out by Larkin,<sup>31</sup> the long-wave deformations of the FLL are responsible for the loss of long-range order. These are the deformations with wavelengths of the order of (or larger than) the correlation lengths  $R_c$  and  $L_c$ .<sup>32</sup> This concept might break down if  $R_c \approx a_0$ . However, we observed that the onset of the peak always occurred at  $R_c/a_0 \approx 15$ . Moreover, Brandt's computer simulations<sup>20</sup> showed that the concepts of the 2D CP theory also hold for an amorphous FLL ( $R_c \approx a_0$ ). Finally, an experimental argument against the possibility of a sudden increase of  $W(0)$  at  $b_{ST}$  comes from the fact that  $b_{ST}$  depends on  $d$  (see Fig. 3), whereas the coefficient  $C_{dl}(T)$  in Eq. (6) is essentially the same for all samples.<sup>7</sup> Thus,  $W(0)$  does not depend on  $d$ , and therefore cannot be responsible for the peak effect.

### C. Topological defects in the FLL

The pinning force exerted on a vortex lattice strongly depends on the shear modulus. When the vortex lattice becomes softer, it can better adjust itself to the pins and the pinning force becomes larger. Because topological defects locally reduce  $c_{66}$ , they cause  $F_p$  to increase, and may therefore be the reason of the peak effect. Topological defects may develop at elastic instabilities.

For a thin film in a perpendicular field the criterion for an elastic instability in the FLL due to a single very strong pin has been given among others by Brandt:<sup>20</sup>

$$u(0) = Aa_0, \quad (7)$$

where  $u(0)$  is the distortion of the FLL by the action of a line force  $f_l$  in the origin and  $A$  is a constant usually taken to be  $(2\pi)^{-1}$  for overlapping vortices. Below the elastic limit  $u(0)$  is given by<sup>29,5</sup>

$$u(0) = \frac{1}{4\pi} \frac{f_l}{c_{66}} \ln \left[ \frac{w}{a_0} \right], \quad (8)$$

where the appropriate cutoffs are chosen at  $w$  and  $a_0$ . For a very dense system of collectively acting, randomly distributed *weak* pins no criterion for a structural transition has been formulated yet. In this case the net forces

(per unit length) due to many pins per individual flux line form a distribution, supposedly Gaussian, with a variance given by

$$\sigma_f = [(n_v \phi_0 / B) \langle f^2 \rangle / d]^{1/2}. \quad (9)$$

We propose here to identify  $\sigma_f$  with  $f_l$  since, if  $\sigma_f$  fulfills the criterion for single-line pins given by Eqs. (7) and (8), there is a good chance to find somewhere in the FLL a fluctuation sufficiently large to cause a local elastic instability. The latter may generate topological defects upon a uniform movement of the FLL past the pins. Combining Eqs. (5) and (7)–(9), we find at the structural transition

$$\left[ \frac{R_c}{a_0} \right]_{ST} \approx \frac{0.186}{A} \frac{\ln(w/a_0)}{[\ln(w/R_c)]^{1/2}}. \quad (10)$$

Inserting a typical experimental value of 40 nm for  $a_0$ , we obtain  $(R_c/a_0)_{ST} \approx 0.69/A \approx 4.3$  for  $A = (2\pi)^{-1}$ . Most importantly, this result is independent of  $T$ ,  $d$ , or material, in agreement with our experiments as illustrated for a few cases in Fig. 4. This criterion, combined with Eqs. (5) and (6), predicts  $(1 - b_{ST}) \propto d^{-1/2}$  for the same reduced temperature, in good agreement with the data shown in Fig. 3. The slope of the straight line in Fig. 3 corresponds with  $(R_c/a_0)_{ST} \approx 17$ . The numerical disagreement should not be considered as a severe discrepancy for several reasons: (i) the LO theory does not provide a rigorous definition of  $R_c$ , (ii) the arguments used in our model have a statistical character, and (iii) the constant  $A$  is not rigorously defined either. A lower threshold for elastic in-

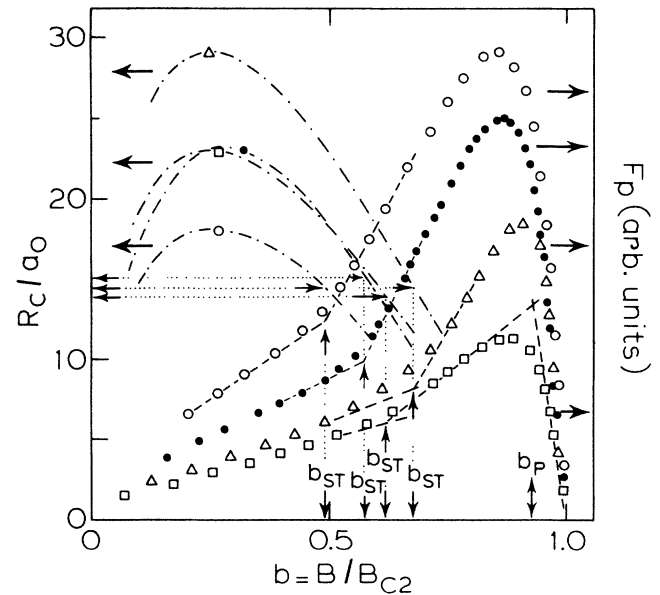


FIG. 4.  $F_p$  and  $R_c/a_0$  vs  $b$  for three  $\text{Nb}_3\text{Ge}$  films and one  $\text{Mo}_3\text{Si}$  sample for comparison.  $\text{Nb}_3\text{Ge}$ : No. 5,  $t=0.46$  (open circles); No. 7,  $t=0.5$  (triangles); No. 6,  $t=0.55$  (squares); and  $\text{Mo}_3\text{Si}$ : No. 8,  $t=0.88$  (solid circles).  $b_{ST}$  and  $b_P$  are defined by the linear extrapolations (dashed lines). Independent of the thickness or temperature a value of about 15 is found for  $(R_c/a_0)_{b_{ST}}$ .

stabilities follows from the computer simulations of Brandt,<sup>20</sup> and Seeger<sup>33</sup> pointed out that the maximum elastic shear distortion of a crystal lattice is 0.05 rather than 0.16 times the lattice parameter. Inverting the procedure, we find from our experimental values of  $b_{ST}$  that the elastic instabilities would be created at a local distortion  $u(0)=0.047a_0$ . Considering the uncertainties mentioned above, this can be only viewed as an indication that topological disorder (FLD's) develops easier than that which follows from the criterion given by Eq. (7) with  $A=(2\pi)^{-1}$ .

#### D. Limited shear strength

In his model for collective pinning Kerchner<sup>2</sup> argues that the limited shear strength of the FLL determines the minimum size of a correlated region. We would like to place this argument in a somewhat different context. The collective pinning theory is a special case of a random-field theory, and is therefore analogous to the random-field theory for magnetic spin systems.<sup>34</sup> One discriminates between continuous symmetry systems where a Bloch wall separates regions of different spin alignment, and Ising systems with sharply defined boundaries. We think the same situation occurs in a FLL. Analogous to a continuous symmetry system is a FLL with only elastic distortions and diffuse boundaries between correlated regions (this is one reason  $R_c$  is not well defined). Analogous to an Ising system is a FLL divided into grains separated by arrays of dislocations as was proposed by Mullock and Evetts.<sup>22</sup> Both descriptions fit the data (see Fig. 4 of Ref. 22); the experiments (Sec. IV) favor the LO description below the peak. The argument for a limited shear strength used in this case would give a crude estimate for the value of  $R_c$  at which the elastic limit is attained. With a typical strain of the order of  $a_0/2R_c$  the shear stress is  $c_{66}a_0/2R_c$ . The flow stress is estimated by Schmucker<sup>35</sup> using Seeger's argument<sup>33</sup> to be  $Ac_{66}$  with  $A$  between  $(2\pi)^{-1}$  and  $\frac{1}{30}$ . This leads to the conclusion that below  $(R_c/a_0)_{FL} \approx 0.5/A$  the FLL starts to deform plastically. It will attain a new equilibrium structure stabilized by the pinning interaction which has become more efficient because of the lattice softening.

In conclusion, we think both mechanisms C and D for the onset of the peak seem to apply equally well and are more or less equivalent. We nevertheless prefer the description in terms of local elastic instabilities because of the more statistical character of the argument which accommodates better with the picture of the collective pinning theory, where pinning is dominated by the fluctuations that occur in pin size and distribution.

Below  $b_{ST}$  the FLL is distorted elastically and pinning is described by the LO theory. Above  $b_{ST}$  it is plastically distorted, so that the size of the correlated regions is smaller than that given by Eq. (5). Mullock and Evetts<sup>22</sup> propose  $V_c \approx D_c^2 d$ , where  $D_c$  is the size of the square array of edge dislocations, and a suggestion by van der Meij and Kes<sup>14</sup> would yield  $V_c \approx D_c^4 d/a_0^2$  in this situation. Irrespective of the structure of the FLL, Eq. (1) holds. Therefore, the volume pinning force of a defective FLL is larger than the LO theory predicts.

### IV. THE EFFECTS OF MAGNETIC FIELD AND TEMPERATURE SWEEPS

In some regions of the magnetic field the pinning force depends essentially on the way the measurements are carried out. Different values of  $F_p$  are found for the CS and CV methods (Sec. II). Temperature and field excursions even have a more pronounced effect. In this section we describe new results obtained by CS and CV  $I_c$  measurements carried out with the appropriate field or temperature sweeps. The resulting history effects reflect the presence of dislocations in the FLL and also confirm the explanation of the peak effect presented in the preceding section.

#### A. Evidence for FLD's

Since  $a_0$  only depends on  $B$ , a fast temperature sweep at constant field would leave the FLL structure unchanged (the relaxation time of the FLL is of the order of seconds). Topological defects present at the starting point of the temperature sweep would be carried over to the new temperature. Depending on the stability, the FLL would either relax to a regular lattice, thereby locally increasing  $R_c$  and  $c_{66}$ , or retain the defects, if this is energetically favorable. The resulting structure of the FLL would correspond to a local minimum of the free energy in configu-

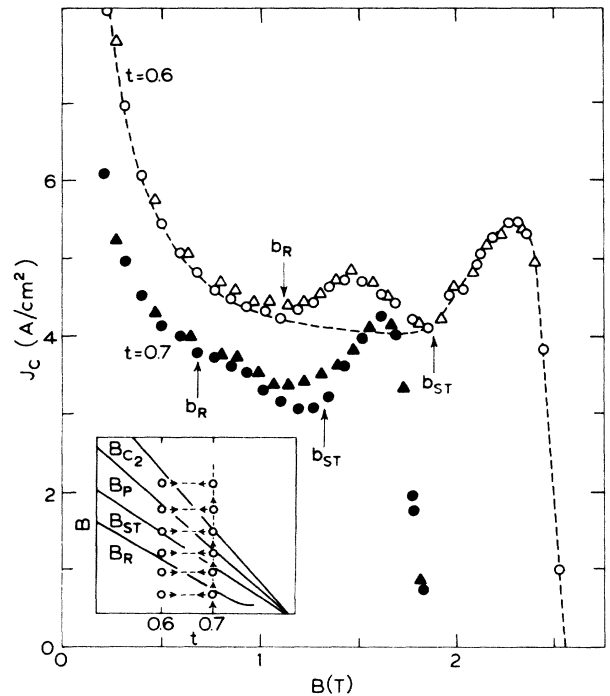


FIG. 5. Isofield experiment for Nb<sub>3</sub>Ge, sample No. 2. The inset schematically shows the way of performing the measurement. After each temperature excursion (horizontal arrows) the vortex lattice is stabilized and  $J_c$  measured (circles). Then the field is increased (vertical arrow). The resulting  $J_c$  values are plotted versus  $B$  for  $t=0.7$  (solid symbols) and  $t=0.6$  (open symbols) in increasing field (circles) and decreasing field (triangles). The results of CS isothermal measurements at  $t=0.6$  are depicted by the dashed line. A distinct second peak can be seen for  $t=0.6$  at fields for which the peak occurs at  $t=0.7$ .

ration space which is not necessarily the lowest one. It might be trapped in a relatively high minimum separated from a lower minimum by an entropy barrier large enough to present a decay on typical experimental time scales. Temperature sweeps thus provide a possibility to demonstrate the existence and the stability of plastic defects of the FLL.

A typical result of such an isofield experiment is given in Fig. 5. For clarity we have plotted  $J_c$  instead of the pinning force versus  $B$ . The inset schematically shows the way the experiment is performed in increasing fields. At the higher temperature ( $0.7T_c$ ) the magnetic field is increased until the first measuring point is reached. The FLL is stabilized by applying the critical current for about 1 min. Subsequently the sample is rapidly (2–3 sec) cooled down to  $0.6T_c$ . The same procedure of stabilizing the vortex structure is used before  $J_c$  is measured at the lower temperature. The film is then warmed up again and after stabilization  $J_c$  at  $0.7T_c$  is recorded. This measuring cycle is carried through for increasing and decreasing field. The  $J_c$  data for  $0.6T_c$  between  $b_R$  and  $b_{ST}$  clearly show an enhancement with respect to the isothermal CS measurements (dashed line in Fig. 5) which agree up to  $b_{ST}$  with the 2D CP prediction. The enhancement indicates a reduction of  $R_c$  below the value given by Eq. (5) (see also discussion of Fig. 8) revealing that the structural disorder belonging to the peak regime at  $0.7T_c$  is carried over to the lower temperature. The conserved disorder turns out to be metastable, since a sufficiently large, additional current causes the enhancement of  $F_p$  to disappear gradually. We can only think of FLD as being responsible for this behavior because elastic deformations would relax during the temperature excursion.

If we carry out the same experiment between  $0.8T_c$  and  $0.6T_c$ , we observe at  $0.6T_c$  two peaks well separated by a region in which the data points and the dashed line exactly coincide. We also studied the effect of a superimposed ac field or ac current on the stability of the structural disorder. The same result as with the additional dc current was observed: For large enough ac amplitudes the conserved disorder disappeared.

We conclude that these results justify the hypothesis of a structural transition at  $b_{ST}$  put forward in the preceding section. For the first time clear experimental evidence is provided that shows that the peak effect is caused by plastic deformations of the FLL. This proves the 2D case only; in three dimensions other mechanisms<sup>1,5</sup> may be responsible, although a structural transition seems possible as well.<sup>22,36</sup>

### B. History effects and structural relaxation of the FLL

Figure 6 shows a closeup of the isothermal CS and CV measurements on  $Nb_3Ge$ , sample No. 2. Between  $b_R$  and  $b_{ST}$  the critical current is history dependent. The magnitude of the hysteresis depends on the kind of measurement (CV or CS), on the temperature, and on the sample preparation. At higher temperature the hysteresis gets smaller, while  $b_{ST} - b_R$  increases (see Fig. 7). The influence of the sample preparation and therefore the number and size distribution of pinning centers has not been sys-

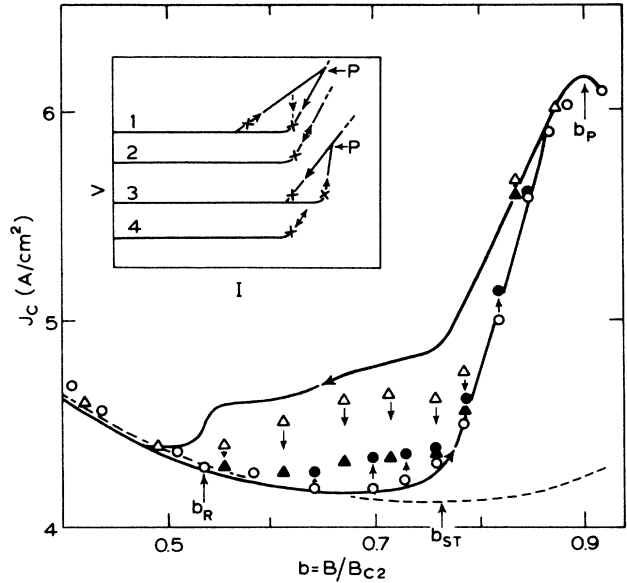


FIG. 6. Isothermal  $J_c$  measurements on  $Nb_3Ge$ , sample No. 2 at  $t=0.7$ , revealing history effects between  $b_R$  and  $b_P$ . Solid lines show results of CV measurements, arrows indicate field directions. Data points depict results of CV  $I$ - $V$  measurements as shown in the inset. Circles: field increased from a value below  $b_R$  initiating a FLL with few FLD's. Triangles: field decreased from  $b_P$  initiating a FLL with many FLD's. Open symbols refer to the first current ramp for the initial FLL structure (curves 1 and 3), solid symbols give  $J_c$  values after current-induced structural relaxation of FLL (curves 2 and 4). The dashed line represents the 2D CP theory. The inset schematically shows the history effects of four measured  $I$ - $V$  curves at a field between  $b_R$  and  $b_{ST}$ . The crosses denote the  $1\text{-}\mu V$  criterion defining  $I_c$ . The voltage at  $P$  is typically of the order of a few mV.

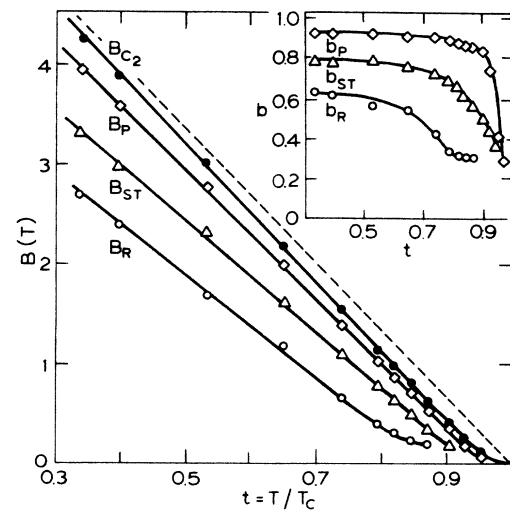


FIG. 7.  $B(T)$  and  $b(t)$  diagrams delineating the characteristic fields separating the different structural phases of the FLL. Below  $B_R$ , elastic deformations only; between  $B_R$  and  $B_{ST}$ , few plastic deformations depending on history; between  $B_{ST}$  and  $B_P$ , many plastic deformations to amorphous; between  $B_P$  and  $B_{c2}$ , amorphous. The dashed line gives  $B_{c2}(T)$  as obtained from the midpoints of the resistive transition in field.

tematically studied so far. It can be said that the Ar-bombarded film (No. 2) showed a more distinct history dependence than the untreated samples, which was the reason for choosing this sample for our discussion.

The inset of Fig. 6 schematically shows four characteristic  $I$ - $V$  curves at a field in the region between  $b_R$  and  $b_{ST}$ . Curve 1 depicts a current sweep after increasing the magnetic field from below  $b_R$ . At small currents the FLL structure is relatively undisturbed, because the FLL "remembers" the structure at the starting field below  $b_R$ . The number of topological defects is small and the critical current is also. This state apparently is not stable in a moving FLL since a further increase of the current causes a decrease of the voltage (dashed vertical line) which indicates a structural change to a more disordered FLL. It seems that FLD's are created when the FLL is drifting through the sample. This current-induced relaxation process takes place within a few seconds depending on  $I - I_c$ , and is therefore probably related to the flux flow velocity. For a continuous current sweep it terminates at  $P$ , where the increasing and decreasing current curves join. Depending on the sweep rate, the voltage at  $P$  is of the order of a few millivolts. The new  $I_c$  value is larger because of the greater disorder. A second current sweep (curve 2) shows that the current-induced state with more defects is a (meta)stable equilibrium state. We cannot decide whether it has a lower energy than the initial state or not.

The opposite process can be observed if the field is decreased from  $b_p$ . At  $b_p$ , where the FLL is strongly disordered, a current larger than  $I_c$  was first applied to define an unambiguous initial condition. Starting with this large disorder a large critical current is measured (curve 3). During flux flow the FLL relaxes to a more stable state producing the steep rise in the  $I$ - $V$  curve just above  $I_c$ . This time the relaxation leads to a removal of FLD's and a lower  $I_c$  value. The new vortex structure is stable as follows from curve 4. It is important to prepare the FLL structure unambiguously. For instance, if one measures curve 3 of the inset after a field excursion in zero current starting at a low field, raising it up to  $b_p$  and going back to the measuring field without establishing a well-defined flux-line configuration, one measures a smaller critical current. The data points in Fig. 6 depict the  $J_c$  values obtained in the way described for curves 1 and 3. They can be compared with the results of the CV measurement (solid lines) and the 2D CP theory (dashed line). We note the following points.

(i) Below  $b_R$  no history dependence is observed; there is good agreement with the theory. Therefore the FLL is predominantly elastically distorted.

(ii) Above  $b_{ST}$  plastic deformations contribute essentially to the flux pinning; the history effect is small or absent.

(iii) Between  $b_R$  and  $b_{ST}$  the current-induced state (solid symbols) is independent of history; it apparently is the structure with the lowest attainable free energy in a moving FLL. It is only obtained if the FLL moves sufficiently fast. Going from  $b_R$  to  $b_{ST}$ , FLD's contribute increasingly to the disorder. The temperature dependence of the characteristic fields is given in the phase diagram of Fig. 7. Close to  $T_c$  the  $B_{c2}$  curve shows an upturn, which is due to our definitions of  $B_{c2}$  and  $T_c$  as the

values, where  $\rho(T)$  extrapolates to zero. Defining  $B_{c2}$  and  $T_c$  at the midpoint of the resistive transition would yield the dashed line in Fig. 7 which demonstrates the often observed linear behavior up to  $T_c$ .<sup>37-39</sup>

(iv) The dynamical measurements in decreasing field yield larger  $J_c$ 's than obtained from the  $I$ - $V$  curves (open triangles). In the first case the FLL moves continuously along the pinning centers with a velocity in accordance with the  $1\text{-}\mu\text{V}$  criterion. In the second case the fields of measurement are attained in zero current starting from a partly amorphous FLL. This suggests that for increasing lattice parameter  $a_0$  in going from much to less disorder, more defects are retained in a slowly moving FLL than in a static lattice. The effect is not seen in increasing field for growing disorder and decreasing  $a_0$ .

Some of these characteristics are also seen in Fig. 8, where we show the results of the temperature sweep experiment of Fig. 5, now in a plot of  $R_c/a_0$  versus  $B$ . The points represent the isofield data as a function of increasing (circles) and decreasing (triangles) field. The lines show the results of the isothermal, CV measurements (arrows indicate the field variation).  $R_c$  is obtained from Eqs. (1) and (5), extrapolating  $W(0)$  determined for  $b < b_R$  according to Eq. (6). We note that for fields beyond the maxima the FLL at the lower temperature is less disordered. Except for  $T \approx T_c$ , this follows from theory if the temperature dependences of  $c_{66}$  and  $W(0)$  are taken into account.<sup>7</sup> At constant field the deformation of the FLL decreases with decreasing temperature, because  $c_{66}$  increases more rapidly than  $f_p$ . The FLL becomes relatively stiffer. In general, we see in Fig. 8 that by going from  $0.6T_c$  to  $0.7T_c$  (increasing disorder)  $R_c/a_0$  coincides with the increasing field curve and the opposite is observed if disorder is decreased. The curves of the CV measurements seem to determine the limits of attainable  $R_c/a_0$  values at a certain temperature. During a tem-

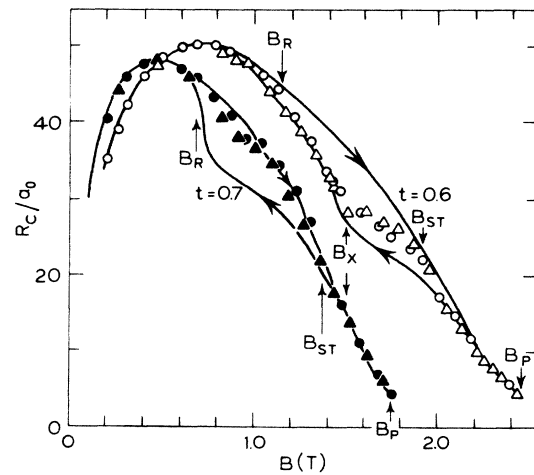


FIG. 8. Plot of  $R_c/a_0$  vs  $B$  for  $\text{Nb}_3\text{Ge}$ , sample No. 2 at  $t = 0.6$  and  $0.7$ . The CV measurements (solid lines) (field direction indicated by arrows) are compared with the isofield measurements for increasing (circles) and decreasing (triangles) field as given in Fig. 6.  $B_x$  marks the field at which the isofield data deviate from the solid line at  $t = 0.6$ . It coincides with the field at which the solid lines at  $t = 0.7$  rejoin.



perature sweep the FLL tends to keep the order or disorder once present.

Above the field  $b_x$  a somewhat different behavior is found for  $t=0.6$ , where the  $R_c/a_0$  data gradually approach the increasing field curve which represents the more ordered state. The field  $b_x$  marks the point at which in Fig. 5 the maximum in the first peak for  $0.6T_c$  is observed and at which for  $0.7T_c$  the  $J_c$  curves for increasing and decreasing fields rejoin and  $d^2J_c/db^2$  changes sign. This might be a coincidence, but we also found it for the other temperature sweep experiments we did. A possible explanation may be that the FLL structure between  $b_{ST}$  and  $b_p$  gradually changes from one with many well-defined topological defects (up to  $b_x$ ) to a more amorphous structure in which dislocations are difficult to define. This would also explain why cooling down in a field larger than  $B_p(0.7)$  always leads to  $J_c$  values in accordance with the increasing field curve.

## V. SUMMARY

A combination of CV and CS  $I_c$  measurements has proved to be a useful tool for the detection of structural changes of the FLL.  $I$ - $V$  curves starting from a well-defined FLL structure directly reflect relaxation processes, times, and directions of the FLL at a given temperature and field. The CV method provides a suitable way of recording  $F_p$  belonging to the unrelaxed vortex structure.

Our experiments on amorphous  $Nb_3Ge$  films ( $d < 3 \mu m$ ) showed that the 2D CP theory is valid for an elastically deformed FLL and that the peak beyond  $b_{ST}$  is caused by an increasing number of plastic defects in the vortex structure. These FLD's lead to a decrease of  $c_{66}$  and  $R_c$ . The enlarged pinning force cannot be fitted by a

modified scaling law consistent with the LO theory. Much better agreement is obtained if  $V_c$  is determined by a FLD model.<sup>22</sup> At the field  $B_{ST}$  the local elastic limit of the FLL in the presence of pins is reached and a structural transition from a mainly elastically to a plastically distorted lattice occurs. The field  $B_{ST}$  can be deduced from Eq. (5) and the criterion for the elastic limit derived in Sec. III C. Our experiments on  $Nb_3Ge$  and  $Mo_3Si$  revealed the size of the correlated regions at the structural transition to be about  $15a_0$ . This indicates that local distortions in the FLL of the order of  $0.05a_0$  might be sufficient to produce topological defects.

Temperature and field sweeps reveal a history dependence of  $J_c$  between the reduced fields  $b_R$  and  $b_p$ . It is caused by the metastable vortex structure which tends to keep the order or disorder once present. Between  $b_R$  and  $b_p$  this is energetically allowed. Sufficiently fast vortex motion leads to a structural relaxation to the stable state.

The study of the effects described here might also be of importance to the understanding of pinning and history phenomena in other two-dimensional systems, e.g., charge density waves.<sup>40</sup> In fact, the intrinsic properties of a FLL make it a unique 2D model system, because the lattice parameter, the elastic interaction, and the pinning strength can be changed at will by varying the magnetic field and the temperature.

## ACKNOWLEDGMENTS

We wish to thank E. H. Brandt, J. A. Mydosh, and P. Horn for stimulating conversations. L. Attanasio and A. Pruijboom are gratefully acknowledged for the preparation of the samples, and F. Munnik for experimental assistance.

<sup>1</sup>A. I. Larkin and Yu. N. Ovchinnikov, *J. Low Temp. Phys.* **34**, 409 (1979).

<sup>2</sup>H. R. Kerchner, *J. Low Temp. Phys.* **50**, 335 (1983).

<sup>3</sup>R. Labusch, *Cryst. Lattice Defects* **1**, 1 (1969).

<sup>4</sup>A. M. Campbell, *Philos. Mag. B* **37**, 149 (1978).

<sup>5</sup>R. Schmucker and E. H. Brandt, *Phys. Status Solidi B* **79**, 479 (1977).

<sup>6</sup>H. R. Kerchner, *J. Low Temp. Phys.* **46**, 205 (1982).

<sup>7</sup>P. H. Kes and C. C. Tsuei, *Phys. Rev. B* **28**, 5126 (1983); *Phys. Rev. Lett.* **47**, 1930 (1981).

<sup>8</sup>In Ref. 7 the field at which the peak sets on was called  $b_{RN}$ .

<sup>9</sup>N. Toyota, A. Inoue, T. Fukase, and T. Masumoto, *J. Low Temp. Phys.* **55**, 393 (1984).

<sup>10</sup>S. Yoshizumi, W. L. Carter, and T. H. Geballe, *J. Non-Cryst. Solids* **61&62**, 598 (1984).

<sup>11</sup>E. J. Osquiguil, V. L. P. Frank, and F. de la Cruz, *Solid State Commun.* **55**, 227 (1985).

<sup>12</sup>H. R. Kerchner, D. K. Christen, C. E. Klabunde, S. T. Sekula, and R. R. Coltmann, Jr., *Phys. Rev. B* **27**, 5467 (1983).

<sup>13</sup>R. Meier-Hirmer, H. K pfer, and H. Scheuer, *Phys. Rev. B* **31**, 183 (1985).

<sup>14</sup>G. P. van der Meij and P. H. Kes, *Phys. Rev. B* **29**, 6233 (1984).

<sup>15</sup>B. D. Lauterwasser and E. J. Kramer, *Phys. Lett.* **53A**, 410

(1975), and references cited therein concerning the peak effect.

<sup>16</sup>H. K pfer and W. Gey, *Philos. Mag.* **36**, 859 (1977), and references cited therein concerning the history effect.

<sup>17</sup>A. B. Pippard, *Philos. Mag.* **19**, 220 (1969).

<sup>18</sup>In Ref. 7 it has been discussed that 2D melting cannot be responsible for the peak effect.

<sup>19</sup>P. H. Kes, R. W rdenweber, and C. C. Tsuei, in *Proceedings of the 17th International Conference on Low Temperature Physics, Karlsruhe, 1984*, edited by U. Eckern, A. Schmid, W. Weber, and H. W hl (North-Holland, Amsterdam, 1984), p. 457.

<sup>20</sup>E. H. Brandt, *Phys. Rev. Lett.* **50**, 1599 (1983); *J. Low Temp. Phys.* **53**, 41 (1983); **53**, 71 (1983).

<sup>21</sup>H. Tr uble and U. Essman, *Phys. Status Solidi* **25**, 373 (1968).

<sup>22</sup>S. J. Mullock and J. E. Evetts, *J. Appl. Phys.* **57**, 2588 (1985).

<sup>23</sup>Y. Anjaneyulu, W. C. H. Joiner, J.-L. Lee, and K. Sission, *J. Appl. Phys.* **54**, 3310 (1983).

<sup>24</sup>C. C. Tsuei, in *Superconducting Materials Science*, edited by S. Foner and B. Schwartz (Plenum, New York, 1981), p. 735.

<sup>25</sup>E. H. Brandt, *J. Low Temp. Phys.* **28**, 263 (1977); **28**, 291 (1977); *Phys. Status Solidi B* **77**, 551 (1976).

<sup>26</sup>P. H. Kes and R. W rdenweber (unpublished).

<sup>27</sup>D. K. Christen (private communication).



- <sup>28</sup>E. H. Brandt, J. Low Temp. Phys. **26**, 709 (1977); **26**, 735 (1977).
- <sup>29</sup>A. M. Campbell and J. E. Evetts, Adv. Phys. **21**, 199 (1972).
- <sup>30</sup>E. J. Kramer, J. Nucl. Mater. **72**, 5 (1978); J. Appl. Phys. **49**, 742 (1978).
- <sup>31</sup>A. I. Larkin, Zh. Eksp. Teor. Fiz. **58**, 1466 (1970) [Sov. Phys.—JETP **31**, 784 (1970)].
- <sup>32</sup>It may be worth noting that in case of *flux flow* in the presence of an rf field wavelengths of the order of  $a_0$  are of importance (see A. I. Larkin and Yu. N. Ovchinnikov, Zh. Eksp. Teor. Fiz. **65**, 1704 (1973) [Sov. Phys.—JETP **38**, 854 (1974)]; A. T. Fiory, Phys. Rev. B **7**, 1881 (1973); **7**, 5040 (1973)).
- <sup>33</sup>A. Seeger, in *Handbuch Physik* (Springer, Berlin, 1958), Vol. VII, p. 2.
- <sup>34</sup>Y. Imry and S. K. Ma, Phys. Rev. Lett. **35**, 1399 (1975).
- <sup>35</sup>R. Schmucker, Philos. Mag. **35**, 431 (1977).
- <sup>36</sup>Yu. N. Ovchinnikov, Zh. Eksp. Teor. Fiz. **82**, 2020 (1982); **84**, 237 (1983) [Sov. Phys.—JETP **55**, 1162 (1982); **57**, 136 (1983)].
- <sup>37</sup>M. A. Paalanen and A. F. Hebard, Appl. Phys. Lett. **45**, 494 (1984).
- <sup>38</sup>G. E. Zwicknagl and J. W. Wilkins, Phys. Rev. Lett. **53**, 1276 (1984).
- <sup>39</sup>M. Tenhover and W. L. Johnson, Physica **108B**, 1221 (1981).
- <sup>40</sup>P. A. Lee and T. M. Rice, Phys. Rev. B **19**, 3970 (1979); D. S. Fisher, *ibid.* **31**, 1396 (1985).